Atmos. Chem. Phys. Discuss., 11, 2503–2547, 2011
www.atmos-chem-phys-discuss.net/11/2503/2011/
doi:10.5194/acpd-11-2503-2011

Atmospheric Chemistry and Physics Discussions

Better constraints on sources of carbonaceous aerosols using a combined ^{14}C – macro tracer analysis in a European rural background site

S. Gilardoni[1], E. Vignati[1], F. Cavalli[1], J. P. Putaud[1], B. R. Larsen[2], M. Karl[3], K. Stenström[4], J. Genberg[4], S. Henne[5], and F. Dentener[1]

[1]European Commission, Joint Research Center, Institute for Environment and Sustainability, Ispra, Italy
[2]European Commission, Joint Research Center, Institute for Health and Consumer Protection, Ispra, Italy
[3]NILU, Norwegian Institute for Air Research, Kjeller, Norway
[4]Lund University, Department of Physics, Division of Nuclear Physics, Lund, Sweden
[5]EMPA, Swiss Federal Laboratories for Materials Science and Technology, Dübendorf, Switzerland

Received: 30 November 2010 – Accepted: 16 January 2011 – Published: 24 January 2011

Correspondence to: E. Vignati (elisabetta.vignati@jrc.ec.europa.eu)

Published by Copernicus Publications on behalf of the European Geosciences Union.

ACPD
11, 2503–2547, 2011

Abstract

The source contributions to carbonaceous $PM_{2.5}$ aerosol were investigated at a European background site at the edge of the Po Valley, in Northern Italy, during the period January–December 2007. Carbonaceous aerosol was described as the sum of eight source components: primary (1) and secondary (2) biomass burning organic carbon, biomass burning elemental carbon (3), primary (4) and secondary (5) fossil fuel burning organic carbon, fossil fuel burning elemental carbon (6), primary (7) and secondary (8) biogenic organic carbon. The concentration of each component was quantified using a set of macro tracers (organic carbon OC, elemental carbon EC, and levoglucosan), micro tracers (arabitol and mannitol), and ^{14}C measurements. This was the first time that ^{14}C measurements were performed on a long time series of data able to represent the entire annual cycle. This set of 6 tracers, together with assumed uncertainty ranges of the ratios of OC-to-EC, and the fraction of modern carbon in the 8 source categories, provides strong constraints to the source contributions to carbonaceous aerosol. The uncertainty of contributions was assessed with a Quasi-Monte Carlo (QMC) method accounting for the variability of OC and EC emission factors, and the uncertainty of reference fractions of modern carbon.

During winter biomass burning composed 50% of the total carbon (TC) concentration, while in summer secondary biogenic OC accounted for 45% of TC. The contribution of primary biogenic aerosol particles was negligible during the entire year. Moreover, aerosol associated with fossil fuel burning represented 26% and 43% of TC in winter and summer, respectively. The comparison of source apportionment results in different urban and rural areas showed that the sampling site was mainly affected by local aerosol sources during winter and regional air masses from the nearby Po Valley in summer. This observation was further confirmed by back-trajectory analysis applying the Potential Source Contribution Function method to identify potential source regions. The contribution of secondary organic aerosol (SOA) to the organic mass (OM) was significant during the entire year. SOA accounted for 23% and 83% of OM during

ACPD

11, 2503–2547, 2011

winter and summer, respectively. While the summer SOA was dominated by biogenic sources, winter SOA was mainly due to biomass and fossil fuel burning. This indicates that the oxidation of intermediate volatility organic compounds co-emitted with primary organics is a significant source of SOA, as suggested by recent model results and Aerosol Mass Spectrometer measurements in urban regions. Comparison with previous global model simulations, indicates a strong underestimate of wintertime primary aerosol emissions in this region.

1 Introduction

Recently, the impacts of atmospheric aerosol on climate and human health have led to more intensive efforts to characterize particle matter (IPCC, 2007; Pope and Dockery, 2006; Nel, 2005). Long-term measurements have shown that the European legislation has effectively succeeded in reducing $PM_{2.5}$ concentrations over the last decade, still the concentration of carbonaceous aerosols remained unchanged.

Carbonaceous aerosol is an ubiquitous and significant component of atmospheric aerosol; it accounts for 20 to 50% of the $PM_{2.5}$ mass in urban and rural locations, and up to 70% of the PM_1 mass (Zhang et al., 2007; Querol et al., 2009). In the following years strategies to mitigate carbonaceous aerosol emissions will be necessary to control and lower aerosol concentrations. To achieve this, a better knowledge of carbonaceous aerosol sources on a regional scale is mandatory.

Molecular and elemental tracers have been used to identify the contribution of one or several aerosol sources. Nevertheless, the sources of carbonaceous aerosol, and organic aerosol in particular, are far from being completely and accurately characterized by tracer methods, especially for the difficulties to quantify secondary organic aerosol (SOA), which represents a significant fraction of organic mass. Field measurements have shown that oxygenated organic aerosol (OOA), of which a major fraction is SOA, composes on average 63% of submicron organic mass in urban locations and 83% downwind of urban areas (Zhang et al., 2007).

ACPD
11, 2503–2547, 2011

Tracer methods apportion primary carbonaceous aerosol sources based on the knowledge of chemical profile of each single source and the unapportioned mass is then assigned to SOA (Stone et al., 2008; El Haddad et al., 2010). The uncertainty of SOA concentration is large because it is affected by the sum of each primary source uncertainties. Other authors use the elemental carbon (EC) to organic carbon (OC) ratio to account for SOA mass and then explain the remaining aerosol mass by tracer analysis (Docherty et al., 2008; Yu et al., 2009). This method assumes that OC is emitted only by combustion sources and that the OC to EC ratio of primary emissions is well-known (Yu et al., 2009). This last assumption is seldom verified, since literature OC to EC ratios range over one order of magnitude, and when the ratio is empirically measured, it might be affected by sampling artifacts, and might not represent the variety of carbon sources and meteorology (Lee et al., 2010).

More recently source apportionment studies have been integrated with ^{14}C measurements to distinguish fossil from non-fossil carbon (Szidat et al., 2007; Hodzic et al., 2010). Fossil carbon is produced by fossil material use like fossil fuel combustion, while non-fossil carbon is carbonaceous aerosol with contemporary origin, like biogenic aerosol or biofuel combustion aerosol.

The isotope ^{14}C is formed in the upper troposphere and layers above mainly following the absorption of cosmic ray-produced neutrons by nitrogen atoms (Lal and Peters, 1967). The ^{14}C produced is quickly oxidized to carbon dioxide which is spread throughout the atmosphere and is taken up by plants through photosynthesis. Thus, atmospheric values of contemporary ^{14}C are incorporated into all land-living organisms. When an organism dies, the exchange of carbon with the surrounding environments ends and the $^{14}C/^{12}C$ ratio starts decreasing following the slow radioactive decay (half-life of about 5700 years) of the ^{14}C isotope. This decay is slow compared to the life time of organisms, but it is fast compared to fossil material time scale. As a consequence, the $^{14}C/^{12}C$ ratio in fossil fuels is zero and the isotopic ratio of atmospheric aerosol depends on the relative contribution of fossil and non-fossil carbon.

ACPD
11, 2503–2547, 2011

When radiocarbon data are combined with tracer measurements, they allow the discrimination of anthropogenic from natural, and primary from secondary aerosols (Gelencser et al., 2007; Ding et al., 2008; Lee et al., 2010).

In this paper we present a source apportionment study, focused on carbonaceous aerosol, which combines macro-tracers (OC, EC, and levoglucosan), micro-tracers (arabitol and mannitol), and ^{14}C measurements to explain both primary and secondary components of atmospheric carbonaceous aerosol. Tracers were used to apportion primary carbon, while ^{14}C data allowed us to distinguish fossil from non-fossil carbon. Carbon associated to secondary organic aerosol was calculated by combination of primary/secondary and fossil/non-fossil data.

To solve the source apportionment problem using macro-tracers, micro-tracers, and carbon isotopic ratio we need to know for each source the corresponding emission factors and the reference fraction of modern carbon corresponding to the non-fossil sources. Due to the large variability that characterizes these input parameters, we decided to use a statistical approach. Gelencser et al. (2007) and Szidat et al. (2009) used Latin Hypercube Sampling to calculate a large number of combinations of these input variables and solve the problem. We used instead a Quasi-Monte Carlo (QMC) approach; this method does not require to define a-priori the number of combinations of input variables, but defines this number according to the convergence of the solutions, leading to a more efficient (less time-consuming) algorithm. In addition, with the QMC we introduced the dependency of two input variables: the reference fraction of aerosol modern carbon and the reference fraction of biomass burning aerosol.

To the best of our knowledge, this was the first time that radiocarbon analysis and tracer measurements were applied to such a large dataset. This guarantees the representativeness of results and the significance of seasonal differences. The QMC approach allowed the quantification of the carbonaceous aerosol sources, and at the same time the effect of the input parameter variability on the uncertainty of the apportionment results.

ACPD
11, 2503–2547, 2011

2 Methods

2.1 Aerosol sampling

Aerosol sampling was performed at the Joint Research Centre station for atmospheric research in Ispra, at a background site located to the northwest edge of the Po Valley in northern Italy (45°48′52″ N, 8°38′10″ E, 209 m a.s.l.). The distance from major anthropogenic emission sources is larger than 10 km. The main urban areas around the site are Varese to the east (at 20 km), Novara to the south (at 40 km), and Milan to the south-east (at 60 km). The site was recently characterized and compared with other European rural and remote background sites, and it was categorized as a typical background site in an environment generally strongly affected by anthropogenic emissions (Henne et al., 2010).

The site has been running under the European Monitoring and Evaluation Program (EMEP) since 1985. Measurements include meteorological parameters, aerosol scattering and absorption, particle number size distribution, and gas-phase species concentration (O_3, SO_2, NO_x, and CO). Since 2000 aerosol mass, organic and elemental carbon, and major inorganic ions have been routinely measured in the aerosol phase. Results presented in this paper refer to carbonaceous aerosols collected during 2007.

24-h fine aerosol samples ($PM_{2.5}$) were collected daily from 08:00 a.m. at 1 m^3 h^{-1} on 47 mm quartz filters, and were stored at 4 °C until the analysis. Filters were not pre-heated prior to analysis. Filters were weighted before and after the exposure at 50% and 20% relative humidity in a controlled atmosphere glove box.

2.2 Carbonaceous aerosol measurements

One punch (1 cm^2) of each quartz filter was analyzed to measure organic carbon (OC) and elemental carbon (EC) concentration. OC and EC were measured by thermal-optical analysis with a Sunset Laboratory dual optical carbonaceous analyzer (Birch and Cary, 1996); the thermal evolution protocol EUSAAR-1 was followed (Cavalli et al.,

ACPD
11, 2503–2547, 2011

2010). Quality control was performed with routine measurements of samples prepared with standard sucrose solution and the instrument was periodically calibrated with CO_2.

A subset composed of 48 daily $PM_{2.5}$ aerosol samples was further analyzed to measure tracers of primary biomass burning (levoglucosan) and primary biogenic aerosol (arabitol and mannitol), and to measure ^{14}C content. The samples were chosen according to the following criteria: to represent both cold and warm season, to represent both week days and week–end days, and to have a total carbon (TC) loading large enough to perform tracer and ^{14}C analysis.

Levoglucosan (1,6-anhydro-β,d-glucopyranose) has been measured in atmospheric aerosol where it has been identified as a prevalent organic compounds in smoke from biomass combustion (Fraser and Lakshmanan, 2000; Nolte et al., 2001; Zdráhal et al., 2002; Simoneit et al., 2004; Dixon and Baltzell, 2006). Although other sources have been discussed for atmospheric emissions of levoglucosan such as combustion of lignites (Fabbri et al., 2009) and char/charcoal (Kuo et al., 2008), these are not relevant for the site of the present study. Hence, in this case levoglucosan seems to be a reasonable choice for a specific tracer for biomass combustion. Moreover, the atmospheric stability of levoglucosan was verified by the good correlation with non-dust soluble potassium, an inorganic tracer of biomass burning ($r^2 = 0.73$).

Arabitol and mannitol have been proposed as tracers of fungal spore emissions, and thus of primary biological aerosol particles (PBAP), according to Bauer et al. (2008a). Although it has been reported that saccharides (including arabitol and mannitol) may be emitted during wood burning (Jia et al., 2010; Schmidl et al., 2008a), the concentrations of these species peaked in March and April, while levoglucosan concentration started decreasing; for this reason we exclude a significant influence of biomass burning on these tracer concentrations.

For the analysis of levoglucosan, arabitol, and mannitol a method was implemented, based upon positive electrospray ionization mass spectrometry (Wan and Yu, 2006). Punches of 2 cm^2 were extracted for 7 minutes by ultrasonic treatment in methanol. The solvent was evaporated to near dryness by a mild flow of N_2, and the residue

ACPD
11, 2503–2547, 2011

was dissolved in 250 µL, water containing 18% methanol and 2mM aqueous ammonium acetate. Aliquots (50 µL) were analyzed by high performance liquid chromatography mass spectrometry (HPLC-MS) using a 25 cm × 4.6 mm Prevail Carbohydrate, 5 µm column and a Themo Ion-trap atmospheric pressure LCQ mass spectrometer. The mobile phase was composed of 20% 10mM aqueous ammonium acetate, 8% methanol, and 72% water. Arabitol, levoglucosan, and mannitol were analyzed as ammonium adducts $[M+NH_4]^+$ and quantified by comparison to external standards; signals used for their quantification were *m/z* 170, *m/z* 180, and *m/z* 200, respectively. The precision of the method was evaluated by multiple extractions and injections to be better than 10%. There is no interference with other compounds with the exception of isomeric forms of levoglucosan, such as the monosaccharide anhydrides mannosan (1,6-anhydro-β,d-mannopyranose and galactosan (1,6-anhydro-β,d-galactopyranose), whose contribution is proved to be lower than 10% (Ma et al., 2010).

2.3 Radiocarbon measurements

The carbon isotopic ratio of the non-fossil carbon in atmospheric aerosol has been affected by the nuclear bombing tests that took place during the late 1950's and early 1960's. The ^{14}C level of atmospheric CO_2 almost doubled momentarily during the tests. Since the test ban in 1963, the atmospheric $^{14}C/^{12}C$ ratio has decreased due to the uptake of CO_2 in the oceans and the biosphere and due to fossil fuel ^{14}C-free CO_2 input. The bomb-pulse in atmosphere at clean-air sites at different latitudes has been extensively studied and monitored (Levin and Kromer, 2004; Levin et al., 2008). At present the atmospheric $^{14}CO_2$ is still elevated compared to the natural reference level; in 2006 the enrichment was about 5% (Levin et al., 2008). Environmental ^{14}C measurements are often expressed as the ^{14}C activity of the sample related to that of the international standard for modern carbon (Currie et al., 1989). This ratio is called "fraction of modern carbon" and is denoted f_M.

ACPD
11, 2503–2547, 2011

The same subset of samples as used for the tracer estimation was analyzed for ^{14}C. Prior to the ^{14}C measurements, 50–150 µg of carbon were extracted from the part of the residual filter area according to the principles described by Genberg et al. (2010). The ^{14}C content was quantified using the Lund University single-stage accelerator mass spectrometer (SSAMS) facility (Skog, 2007; Skog et al., 2010). Results are expressed in units of fraction of modern carbon, f_M.

The concentration of non-fossil carbon was calculated as the fraction of modern carbon (f_M) multiplied by the concentration of carbon (TC) and divided by the reference fraction of non fossil carbon ($f_{M(non-fossil)}$), which takes into account the nuclear bomb enrichment and the different content of ^{14}C of biomass burning and biogenic aerosol; in fact, carbonaceous aerosol from biomass burning is further enriched in ^{14}C than biogenic aerosol, because of the older age of burnt wood.

2.4 Source apportionment of carbonaceous aerosols

Carbonaceous aerosol was described as composed of the following 8 categories: primary OC from biomass burning (POC_{bb}), EC from biomass burning (EC_{bb}), primary OC from fossil fuel burning (POC_{ff}), EC from fossil fuel burning (EC_{ff}), primary OC from biogenic sources (POC_{bio}), secondary OC from biomass burning (SOC_{bb}), secondary OC from fossil fuel burning (SOC_{ff}), and secondary OC from biogenic sources (SOC_{bio}). We assumed that these categories include all major sources of carbonaceous aerosol in the troposphere.

POC_{bb} and EC_{bb} are emitted by combustion of biomass, that around Ispra includes wood burning for residential heating in winter and episodic agricultural waste burning at the beginning of fall. During incomplete combustion of biomaterial, such as wood for residential heating, pyrolytic processes may lead to the formation of a number of compounds deriving from cellulose such as levoglucosan. POC_{bb} was inferred from the concentration of levoglucosan and EC_{bb} was calculated assuming a constant EC to OC ratio for primary biomass burning emissions.

ACPD
11, 2503–2547, 2011

$$POC_{bb} = [\text{levoglucosan}] \cdot k_1 \quad (1)$$

$$EC_{bb} = \frac{POC_{bb}}{k_2} \quad (2)$$

where k_1 and k_2 are the OC to levoglucosan and OC to EC emission ratios of biomass combustion, respectively.

POC_{ff} and EC_{ff} are emitted directly from combustion of fossil fuel including residential heating in winter, traffic and industrial processes during the entire year. EC_{ff} was inferred from the total EC concentration after subtraction of EC_{bb}, while POC_{ff} was calculated from EC_{ff} using the expected OC to EC ratio for primary fossil fuel combustion emissions (k_3).

$$EC_{ff} = [EC] - EC_{bb} \quad (3)$$

$$POC_{ff} = EC_{ff} \cdot k_3 \quad (4)$$

POC_{bio} is the OC associated to PBAP, which include viable organisms, dead cells and cell fragments, such as pollen, bacteria, spores, plant debris, and viruses. The size of biological particles ranges over three orders of magnitude. Pollen grains, fragments of plants and animals are typically larger than 10 µm and their contribution to fine aerosol is negligible. On the contrary, spores can be smaller than 10 µm, bacteria can be as small as 1 µm, and viruses range around 100 nm (Matthias-Maser and Jaenicke, 2000). Among these particles only fungal spores seem to contribute significantly to PM_{10} loadings in non-forested areas (Bauer et al., 2008b,a). Still, their contribution to fine aerosol is usually not reported. Arabitol and mannitol, saccharides composed respectively by 5 and 6 carbon atoms, were used as tracers of fungal spore emissions (Bauer et al., 2008a). The number of spores was calculated according to the arabitol and mannitol emission factors reported by Bauer et al. (2008a) and corresponding to 1.2 pg arabitol spore^{-1} and 1.7 pg mannitol spore^{-1}; the content of OC from a single spore was assumed equal to 5.2 pg C spore^{-1}, corresponding to the lower bound reported for PM_{10} aerosol (Bauer et al., 2002).

ACPD
11, 2503–2547, 2011

The contribution of primary biogenic carbon was then calculated according to Eq. (5).

$$POC_{bio} = [\text{number of spores}] \cdot 5.2\ \text{pg OC spore}^{-1} \quad (5)$$

SOC_{ff} and SOC_{bb} correspond to OC produced by the oxidation (e.g. through aging) of intermediate volatility organic compounds (IVOC) and volatile organic compounds from anthropogenic activities (Robinson et al., 2007), while SOC_{bio} is produced by the oxidation of gas-phase biogenic precursors. SOC_{ff} was determined by subtraction of primary carbon associated with fossil fuel (POC_{ff} and EC_{ff}) from the fossil carbon (FC).

$$SOC_{ff} = FC - POC_{ff} - EC_{ff} \quad (6)$$

with

$$FC = [TC] \cdot \left(1 - \frac{f_M}{f_{M(non-fossil)}}\right) \quad (7)$$

where TC is total carbon and $f_{M(non-fossil)}$ being the reference fraction of modern carbon in non-fossil aerosols.

Secondary organic carbon from modern sources (SOC_{bb} and SOC_{bio}) was calculated by the combination of the following two equations:

$$OC = POC_{ff} + POC_{bb} + POC_{bio} + SOC_{ff} + SOC_{bb} + SOC_{bio} \quad (8)$$

$$f_M \cdot [TC] = (POC_{bb} + SOC_{bb} + EC_{bb}) \cdot f_{M(bb)} + (POC_{bio} + SOC_{bio}) \cdot f_{M(bio)} \quad (9)$$

where $f_{M(bb)}$ and $f_{M(bio)}$ are the reference fraction of modern carbon in biomass burning aerosol and biogenic aerosol, respectively. $f_{M(bio)}$ is known from measurements of ^{14}C content in atmospheric CO_2 and it's equal to 1.05 (Levin et al., 2008) in 2006. The discrimation between SOC_{bio} and SOC_{bb} was based on the different reference fraction of modern carbon of biomass and biogenic material. Table 1 summarizes the list of acronyms introduced in this section and the corresponding meaning.

ACPD
11, 2503–2547, 2011

2.5 Solution of the linear equations

2.5.1 Quasi-Monte Carlo approach

To solve the system of linear equations reported in the previous paragraphs we need to make assumptions about the values of the following input parameters: OC to levoglucosan emission ratio of biomass burning (k_1), OC to EC emission ratio of biomass burning (k_2), OC to EC emission ratio of fossil fuel combustion (k_3), $f_{M(bb)}$, and $f_{M(non-fossil)}$.

Due to the variability and uncertainty of these parameters, it would not be defendable to use single values for these parameters. Instead we explored the parameter space using a Quasi-Monte Carlo (QMC) approach to solve the linear equations (Boyle and Tan, 1997), and the 5 input parameters were allowed to vary across the whole uncertainty range reported in Table 2. In a classical Monte Carlo approach, a large number of combinations of the 5 input parameters would be tested and the parameter values would be chosen randomly across the whole variability range. Quasi-Monte Carlo methods reduce the number of combinations needed to represent the parameter space, thanks to the use of deterministic sequence rather than random sequence of values. The deterministic sequences are uniformly dispersed throughout the parameter domain. In this study we used the Sobol algorithm (Sobol, 1967) to create a 5-dimension deterministic sequence. Each point of the sequence, described by 5 coordinates, is a combination of 5 input parameters that can be used to solve the system of linear equations.

The Sobol sequence is a low discrepancy series. This means that any additional point of the series keeps the distribution of sampling points uniform. Thus, we did not need to define a priori the number of sampling points, but we could optimize it to guarantee the solution convergence and to minimize the computational time.

During each iteration of the equation system a new combination of parameters was tested. The maximum number of iterations was set to 100 000 and the convergence was achieved when:

ACPD
11, 2503–2547, 2011

– the number of iterations was at least 10 000,

– the number of non-negative solutions was larger than 1000,

– and the solution estimate varied by less than 1% during the last three iterations.

The QMC method allowed us to calculate for each source during a certain day more than 10 000 solutions, corresponding to more than 10 000 iterations. The frequency with which a certain solution happened, defined the probability of that solution for that specific source during that specific day. As an example, Fig. 1 shows the frequency distribution of QMC solutions corresponding to primary and secondary OC measured on 21 January 2007.

For each daily sample and for each carbon source the probability distribution of the solutions was analyzed to record the 5th, 25th, 50th, 75th, and 95th percentile, as well as the arithmetic mean value. Some combinations of parameters led to negative solutions, meaning negative concentrations. Discarding these outputs, we obtained a smaller solution uncertainty compared to variability of the input parameters.

2.5.2 Input parameter variability range

Literature data indicate that emission ratios depend on nature and properties of fuel and on combustion conditions (i.e. temperature, open burning, contained burning, technology for pollution abatement); in addition, the EC emission factors are further affected by the variability related to the technique used for EC measurements, in fact EC concentration are method specific and can differ widely (Hitzenberger et al., 2006). Based on this dependency and the fact that EC and OC used in this study were measured by thermal-optical technique, the emission ratios here considered include only literature studies based on thermal-optical measurements.

The OC to levoglucosan emission ratios reported in literature range between 1.9 for fireplace combustion of eucalyptus logs (Schauer et al., 2001) and 28 for open burning of agricultural biomass (Hays et al., 2002). Most of the studies refer to wood species

ACPD
11, 2503–2547, 2011

used for domestic heating in the United States (Fine et al., 2001, 2002, 2004) and only limited data exist for European emissions (**?**Schmidl et al., 2008a). The emission ratios measured during burning of wood from central and southern Europe range between 3.7 and 12.7; Puxbaum et al. (2007) recommend the interval 6–7 for contained combustion of European wood. In the present study the range 4–6 was employed since higher values would have led to POC_{bb} larger than the total OC concentration and smaller values are unlikely based on literature data.

OC and EC emission factors of biomass burning and fossil fuel combustion have been recently compiled in the IIASA interim report (Kupiainen and Klimont, 2004) and by the EPA SPECIATE4.1 program last updated in July 2008 (www.epa.gov/ttnchie1/emch/speciation). The compilation indicates that OC to EC ratios of biomass burning range between 0.5 and 69, depending on fuel type and burning conditions, with higher values for leaves and agricultural waste burning (Hays et al., 2002). The range used in the present study (1–20) corresponds to the range 5th–80th percentile of the literature ratios, and it was chosen because it roughly overlaps with the range measured by Colombi et al. (2010) for wood and agricultural burning in northern Italy (1.7–20), which is likely representative for our measurement site.

The OC to EC ratios of fossil fuel burning strongly depends on the technology adopted for combustion and emission abatement. We consider here fossil fuel burning associated to transportation, residential heating, and industrial activities. Although the ratios reported in literature vary between 0.2 for boilers and heavy duty diesel vehicles and 6 for gas vehicles (Kupiainen and Klimont, 2004), values higher than 1.2 were measured only for vehicles used before 2000 (Watson and Chow, 2001; Kupiainen and Klimont, 2007). The variability range used in this study was 0.3–1.2; it comprises the ratio suggested for the overall fossil fuel consumption in the EU15 area (0.7) (Kupiainen and Klimont, 2007), as well as the emission ratio of vehicles in the Milan metropolitan area (60 km south of the sampling site) and measured from tunnel experiments (0.7) (Lonati et al., 2005).

ACPD
11, 2503–2547, 2011

The quantification of primary carbon in this study was based on emission factor ratios measured at dilution ratios relatively high compared to ambient conditions. For example, the emission of carbonaceous aerosol from wood burning is usually determined at dilution ratios of 20 to 45 (Fine et al., 2001, 2002), while ambient conditions correspond to dilution of 1000–10 000. Robinson et al. (2007) showed that primary emissions evaporate significantly upon dilution and the gas-phase species formed by volatilization are then photo-oxidized to produce SOA. Since the majority of emission inventories available so far do not take into account the semivolatile character of primary emissions, the source apportionment results here presented might overestimate the effective primary pollution and underestimate by the same amount the corresponding secondary component.

$f_{M(non-fossil)}$ could not be determined a priori since it depends on the relative contribution of modern carbon sources, e.g. biomass burning and biogenic aerosols, and their reference fractions of modern carbon $f_{M(bb)}$ and $f_{M(bio)}$. $f_{M(bio)}$ is 1.05, while $f_{M(bb)}$ depends on the age of the combusted material and the tree growth rate; for 20–50 year old trees harvested in 1999 Lewis et al. (2004) calculated that $f_{M(bb)}$ varies between 1.13 and 1.31. To account for this uncertainty, $f_{M(bb)}$ and $f_{M(non-fossil)}$ are used as input parameters in the QMC method: $f_{M(bb)}$ was let vary between 1.13 and 1.31, while $f_{M(non-fossil)}$ was let to vary between 1.05 and the value assumed for $f_{M(bb)}$.

2.6 Atmospheric back-trajectories and PSCF analysis

To identify potential source regions for different aerosol fractions we combined the observations with atmospheric back-trajectory calculations. 5-day back-trajectories were calculated every 2 h for the sampling site using the trajectory model FLEXTRA (Stohl et al., 1995). The model was driven by 3-hourly European Center for Medium-range Weather Forecasts (ECMWF) analysis and forecast wind fields with 0.2° × 0.2° horizontal resolution. Trajectories were initialized 50, 100, 200 and 500 m above model ground. The atmospheric boundary layer height along the trajectory path was evaluated using the method described by Stohl et al. (2005). To account for additional vertical mixing in the Alpine terrain the envelope boundary layer height was used (Stohl et al., 2005).

ACPD
11, 2503–2547, 2011

The potential source contribution function (Zeng and Hopke, 1989) defines the probability for an aerosol source of being located in a certain geographical area described by a cell with coordinates (i, j). PSCF at (i, j) was calculated assuming that, if a back-trajectory passes through the atmospheric boundary layer of grid cell i, j, it picks up emissions from that area and transport them to the receptor site. To decide if a back-trajectory was within the atmospheric boundary at grid cell i, j the trajectory altitude was compared with the envelope boundary layer height and trajectory points outside the boundary layer were discarded. The function was defined by the ratio between the number of times that a back-trajectory associated with high concentrations passes through grid cell (i, j) ($m_{i,j}$) and the total number of times that back-trajectories pass through the grid cell (i, j) ($n_{i,j}$), according to the Eq. (10).

$$\mathrm{PSCF}_{i,j} = \frac{m_{i,j}}{n_{i,j}} \cdot w_{i,j} \tag{10}$$

The weight function $w_{i,j}$ was used to reduces the significance of grid cells associated with low trajectory residence times (Pekneya et al., 2004). The function $w_{i,j}$ was defined according to the following formula, where 40 was roughly equal to the 3 times the standard deviation of $n_{i,j}$.

$$w_{i,j} = \begin{cases} 1 & \text{if } n_{i,j} \geq 40; \\ (\frac{n_{i,j}}{40})^3 & \text{if } n_{i,j} < 40; \end{cases}$$

Figure 2 shows per each grid cell the number of back trajectory points within the boundary layer using 100 m as inizialitation altitude; the map, corresponding to the whole year, indicates that the regions affecting the sampling site included the Po Valley to the south – south east, the rural and marine area to the south, and Switzerland to the north.

ACPD
11, 2503–2547, 2011

3 Results and discussion

3.1 Carbonaceous aerosol and tracers

Table 3 reports the average concentration and standard deviation of $PM_{2.5}$ mass, EC and OC corresponding to the daily aerosol samples collected from January till December 2007. The annual $PM_{2.5}$ average was higher than the target value of 25 $\mu g\,m^{-3}$ introduced by the European legislation in January 2010; the target value was exceeded 121 times during the year, indicating a strong influence of regional and local aerosol emission sources. The higher average values during winter (about three times higher than summer averages) were likely due to the contribution of residential heating and the lower mixing layer height that prevented pollutant dilution (Fig. 3a–b). Organic mass (OM), calculated using an OM to OC ratio equal to 1.4, represented 53% and 41% of fine mass during winter and summer, respectively, while the EC contribution was 10% and 7%.

The average $PM_{2.5}$ mass concentration, as well as the average EC and OC concentration for the subset of 48 samples (28 in winter and 20 in summer) selected for tracer and radiocarbon analysis were slightly larger than for the original data set. This was due to the selection criteria based on having enough carbonaceous aerosol to perform multiple tracer analysis and to overcome their detection limits. Student's t-test showed, however, that the subset of samples was representative of the original data set with a 99% significance level for $PM_{2.5}$ mass, OC, and EC.

$PM_{2.5}$ mass, OM, and EC daily concentrations of the subset of 48 samples are reported in Fig. 3b. The concentration of OM and EC averaged 19.4 $\mu g\,m^{-3}$ and 3.5 $\mu g\,m^{-3}$, respectively. The contribution of OM to $PM_{2.5}$ mass varied between 27 and 83%, while EC fraction ranged between 3 and 22%.

Levoglucosan (biofuel/waste burning tracer) was detected in all samples collected during the colder season, while during the warmer period only a small number of samples showed concentrations above detection limit, mainly collected at the beginning of spring and at the end of summer, when environmental conditions were dry enough

ACPD
11, 2503–2547, 2011

to burn biomass waste. The average winter concentration in Ispra (2.8 $\mu g\,m^{-3}$) was higher than the values measured in continental and maritime background European sites (Puxbaum et al., 2007). However, it is comparable to the upper bound of the concentration range measured at European rural sites (i.e. K-puszta, Hungary, and Aveiro, Portugal) (Puxbaum et al., 2007). In relative terms, the winter average contribution of levoglucosan to carbonaceous aerosol in K-puszta and Aveiro was 5 and 9%, respectively (Gelencser et al., 2007), while it reached 10% in Ispra. The percentage contribution measured in the more urbanized Po Valley, at close distance (ca. 50 km) from the measurement site, in winter 2007 and 2009 was 5% (B. R. Larsen, personal communication, 2010).

About one third of the samples was characterized by detectable amounts of saccharides (marker for PBAP), whose concentrations ranged between 2.6 and 31 $ng\,m^3$ for arabitol and from 2.3 to 52 $ng\,m^3$ for mannitol, with the highest values measured at the end of March. These concentrations were smaller than those reported by Bauer et al. (2008a) for an urban site in Vienna, Austria, for PM_{10} samples (arabitol: 7–63 $ng\,m^{-3}$ and mannitol: 8.9–83 $ng\,m^{-3}$), consistently with a bimodal distribution of these species in fine and coarse particles (Kourtchev et al., 2009). The range of arabitol and mannitol concentrations measured in $PM_{2.5}$ aerosol at a rural site in Texas (Jia et al., 2010) were similar to those measured in Ispra.

3.2 Sources of carbonaceous aerosol

For each daily sample and for each carbon source the Quasi-Monte Carlo simulation calculated the frequency distribution of non-negative solutions from all combinations of the input parameters. The average value of this distribution is here considered the best estimate of the carbon source strength. Figure 3c shows the best estimate results for the eight carbon sources described in the experimental section. Note that the OC is not converted into organic mass so the plot does not account for the contribution of atoms other than carbon. Annual and seasonal average carbon concentrations are reported in Table 4.

ACPD
11, 2503–2547, 2011

The single most important carbonaceous aerosol source in Ispra was biomass burning. Although its presence was limited to the colder months, it represented 50% of the total mass of carbon during the whole year. POC_{bb}, SOC_{bb}, and EC_{bb} accounted for 79%, 8%, and 13% of the total biomass burning carbon, respectively. The highest concentrations were measured in January, November, and December, the coldest months of the year. The absence of this source during summer, when dryer weather conditions could facilitate wildfires in the surrounding regions, and the small concentrations during agricultural waste burning season (September and beginning of October) indicate that the main source of biomass burning carbon observed in Ispra was wood burning for residential heating. This conclusion was further supported by the observation that non-dust soluble potassium and levoglucosan concentrations correlated with a slope equal to 0.13, a value closer to fireplace and wood stove emission ratios than to open burning ratios (Puxbaum et al., 2007).

Biogenic carbon was dominated by secondary sources. The contribution of POC_{bio} ranged between 5 and 110 $ng\,m^{-3}$ and was negligible compared to SOC_{bio}, whose concentration ranged from values below 1 $\mu g\,m^{-3}$ in winter up to 7.5 $\mu g\,m^{-3}$ in spring. On average SOC_{bio} represented 8% and 45% of carbonaceous aerosol during winter and summer, respectively, while POC_{bio} contribution was less than 1% in all samples.

Karl et al. (2009) used global chemistry transport model TM5 to evaluate the contribution of secondary biogenic aerosol at Ispra. We compare the result of this source apportionment study with the model output. The SOC_{bio} in summer averaged 3.4 $\mu g\,m^{-3}$, corresponding to 6.1 $\mu g\,m^{-3}$ of organic mass, calculated with the ratio OM to OC equal to 1.8 (Aiken et al., 2008); this concentration agrees well with the average secondary organic aerosol (SOA) concentration (5.4–5.8 $\mu g\,m^{-3}$) simulated by the TM5 during July 2002 in northern Italy (Karl et al., 2009). The model simulation includes the SOA derived from isoprene oxidation and describes as an equilibrium the partitioning of secondary biogenic species between gas and aerosol phase.

From May to August biogenic emissions of e.g. isoprene have been shown to peak at our measurement site (Duane et al., 2002). Daily samples collected during the same

ACPD
11, 2503–2547, 2011

months showed that the mass fraction of biogenic secondary carbon (i.e. SOC_{bio} normalized to the fine aerosol mass) correlated very well with the mass fraction of primary carbon (i.e. the sum of primary OC and EC normalized to fine mass) (Fig. 4), that in summer is emitted exclusively by anthropogenic fossil sources; the good correlation ($r^2 = 0.79$) suggests that larger fractions of anthropogenic primary aerosol offer a larger surface area with chemical affinity for condensation of biogenic gas phase precursors, enhancing secondary biogenic aerosol formation (Bowman and Melton, 2004). A similar enhancement was predicted by CMAQ model in the eastern United States (Carlton et al., 2010).

The equation of the linear fit in Fig. 4 suggests that under the influence of anthropogenic aerosols the biogenic aerosol carbon concentration is doubled compared to an hypothetical condition of zero anthropogenic emissions (on average 2.9 $\mu g\,m^{-3}$ during the period May–August).

Carbonaceous aerosol from fossil fuel combustion was observed both during winter and summer and composed 27% of the total carbon mass. It partitioned into POC_{ff} (22%), SOC_{ff} (32%), and EC_{ff} (46%). Differently from biomass burning, fossil fuel combustion produced a larger amount of elemental carbon relative to primary and secondary organic carbon. Although, the fraction of TC represented by fossil fuel combustion aerosol was higher in summer than in winter, the average concentrations of POC_{ff}, SOC_{ff}, and EC_{ff} during winter were about twice the summer values.

3.3 How source apportionment data explain model/observation disagreement

The global chemistry transport model TM5 (Krol et al., 2005) was employed by Karl et al. (2009) to simulate OM concentration at Ispra during the EMEP intensive campaign from July 2002 to June 2003. Globally, a horizontal resolution of $6^\circ \times 4^\circ$ was used, with a two-way zooming algorithm resolving the European domain at a resolution of $1^\circ \times 1^\circ$. TM5 was coupled with the secondary organic aerosol module developed by Tsigaridis et al. (2006) and linked to the gas-phase chemistry module CMB-IV (Gery et al., 1989). The model underestimated the observation during most time of the year, with the exception of July–August period.

ACPD
11, 2503–2547, 2011

The average OM concentrations measured during the intensive campaign 2002/2003 (16.9 $\mu g\,m^{-3}$ in winter and 6.7 $\mu g\,m^{-3}$ in summer) were comparable to those measured during 2007 within the variability range. The similarity of carbonaceous aerosol concentrations observed during the two periods allowed the comparison of source apportionment results of 2007 with model simulation of 2002/2003.

The OM simulations were divided into POA and SOA contributions. For comparison purposes the measured POA and SOA were calculated according to the following equations:

$$POA = 1.4 \cdot POC_{bb} + 1.8 \cdot POC_{bio} + 1.4 \cdot POC_{ff} \quad (11)$$

$$SOA = 1.4 \cdot SOC_{bb} + 1.8 \cdot SOC_{bio} + 1.4 \cdot SOC_{ff} \quad (12)$$

The OM to OC ratio of biogenic aerosol was assumed equal to 1.8 according to Chen et al. (2009).

The average POA derived from 2007 measurements was 19.0 and 1.6 $\mu g\,m^{-3}$ during winter and summer, respectively. The corresponding model output were 2.3 and 1.5 $\mu g\,m^{-3}$. The model simulated correctly the summer concentration, while the underestimation observed in winter was likely due to the underestimation of biomass burning emission in the model; in fact the POA associated to biomass burning (on average 17.2 $\mu g\,m^{-3}$) was quite similar to the difference between observed and modeled OM.

SOA concentrations derived from source apportionment averaged 9.1 and 8.6 $\mu g\,m^{-3}$ in winter and summer, respectively. Although the model simulated correctly the biogenic SOA during June–August (see Sect. 3.2), it generally underestimated the observations; the average model SOA was 0.8–1 and 3.2–3.4 $\mu g\,m^{-3}$ in winter and summer, respectively. The difference between SOA observed and modeled was likely due to the underestimation of biomass burning and fossil fuel SOA from oxidation of IVCO, as well as underestimation of biogenic SOA during seasons other than summer.

ACPD
11, 2503–2547, 2011

3.4 Uncertainty analysis

The variability of the input parameters used for the QMC calculation led to uncertainty of the simulation results, as reported in Fig. 5 for each day and for each carbon source. As a measure of the uncertainty we used the difference between the 95th and the 5th percentile of the solutions, corresponding roughly to $\pm 2\sigma$.

The uncertainty of POC_{bb} was usually smaller than that of SOC_{bb}; their average values were 10% and 17% of total carbon concentration, respectively. In a few cases (5 samples), when the SOC_{bb} fraction was larger than 12% of TC, its uncertainty was higher than 25%.

Similarly, SOC_{ff} was characterized by a larger uncertainty compared to that of POC_{ff}, especially during winter. POC_{ff} uncertainty ranged between 3 and 15% of TC, while SOC_{ff} uncertainty was often larger than 20%. The highest uncertainties were associated with the highest concentrations during winter.

Both EC_{bb} and EC_{ff} were characterized by uncertainties smaller than 20% during the entire year, and close to zero during summer.

The uncertainty of SOC_{bio} averaged 12%; the few values above 25% were observed when SOC_{bio} percentage was larger than 12% during winter.

The lower uncertainties during summer were due to negligible contribution of biomass burning. When biomass burning carbon was zero, EC to OC emission ratio of fossil fuel combustion was the only input parameters left to affect the simulation output, reducing the uncertainty of primary and secondary fossil fuel OC during summer compared to winter.

Neglecting the distinction between primary and secondary sources, the carbon emitted by biomass burning and fossil fuel burning can be defined by the sum of the corresponding POC and SOC; this results in a reduction of uncertainty. During winter the uncertainty of OC from the biomass and fossil fuel burning averaged 6% and 8% of TC, and the maximum uncertainties were 9% and 18%, respectively.

ACPD
11, 2503–2547, 2011

3.5 Seasonality of carbonaceous aerosol sources in comparison with other studies

We compared the seasonality of the source contribution to carbonaceous aerosols with apportionment data based on ^{14}C and tracer measurements performed at other European urban and rural locations (Table 5); data from remote sites are not reported because these are dominated by biogenic emissions during the whole year (Gelencser et al., 2007).

OC_{bb}, OC_{ff}, and OC_{bio} in Table 5 are equal to the sum of primary and secondary OC. At Aveiro e K-puszta OC_{bb} takes into account only the primary contribution since no distinction was made between secondary biogenic and secondary wood burning OC. During summer the small contribution of OC and EC form biomass burning suggests that the secondary non-fossil OC was a good estimate of OC_{bio}. At Roveredo and Moleno OC_{bb} was assumed equal to non-fossil OC; in fact, aerosol mass spectra acquired during the same study compared very well with wood burning emission, pointing to a insignificant influence of biogenic OC (Szidat et al., 2007).

During winter OC and EC emitted by biomass burning at the rural sites, although characterized by a large variability, were consistently higher than the values reported for the urban sites. Conversely, the contribution of fossil fuel carbonaceous aerosol did not show clear differences. The biomass burning carbon measured in Ispra compared well with the rural measurements and the fossil fuel carbon fraction was consistently lower than that measured in urban sites.

A limited set of measurements were available during the summer season. The contribution of biomass burning was smaller than 11% at all sites. Fossil fuel carbon fraction at the urban sites was about two times larger than the rural fractions, while the biogenic carbon contribution was markedly more significant at the rural locations. The composition of carbonaceous aerosol in Ispra was comparable to that of urban sites; Ispra aerosol had a larger fraction of fossil fuel carbon aerosol relative to the rural locations.

ACPD
11, 2503–2547, 2011

The similarity of the source contribution in Ispra with rural sites in winter and with urban sites in summer was likely due to the influence of urban polluted air masses linked to lower atmospheric stability during summer. To verify this hypothesis, we further investigate the origin of polluted air masses with potential source contribution function (PSCF) for biomass burning and fossil fuel combustion aerosol.

3.6 Source regions

For PSCF purposes, the contribution of a specific carbon source was considered high when the percentage of TC associated to that source was larger than the 75th percentile. We selected samples characterized by high contribution of POC_{ff} and POC_{bb}, limiting the investigation to primary carbon. This limitation was due to the smaller uncertainty of carbon from primary sources compared to secondary ones, and to the fact that the PSCF algorithm calculates the probability associated to primary pollutants transport excluding formation of secondary species.

The POC_{ff} contribution to TC was more significant during summer, while the POC_{ff} fraction was higher during the colder months, especially November and December. As a consequence the PSCF maps of POC_{ff} and POC_{bb} in Fig. 6 shows the influence regions typical of the winter and summer months, respectively. The smaller probability values of POC_{bb} are due to the lower mixing layer height during winter and the consequent lower influence of regional air masses.

The fossil fuel carbon PSCF was higher in the grid cells close to Ispra and close to Milan, indicating a strong contribution from local sources and from regional sources mainly located in the urban areas of Milan and surroundings. The map shows also a likely contribution from the Po Valley region, to the south-east of Milan. This area is characterized by high density of population and industrial activities.

The highest PSCF values of POC_{bb} were observed in the surroundings close to Ispra. The remaining grid cells were characterized by probabilities smaller than 0.2, indicating that the biomass burning primary carbon observed in Ispra was mainly from local sources. The PSCF was larger than 0.1 in rural areas located to the south of

ACPD
11, 2503–2547, 2011

Ispra and to the south-east of Milan, while null values were observed in the areas characterized by higher population density (Fig. 6c). This does not mean that the biomass burning emissions in urban areas were null, but that the influence of these emissions at the receptor site was negligible compared to the local emissions.

4 Conclusions

The sources of carbonaceous aerosols in Ispra, a European background site at the edge of the Po Valley, were investigated using macro-tracers (EC, OC, and levoglucosan), micro-tracers (arabitol and mannitol), and ^{14}C measurements. The concomitant use of tracers specific of a single source and measurements related to multiple sources constrained the source apportionment results. A Quasi-Monte Carlo approach was used to solve the source apportionment problem, reducing in most of the cases the uncertainty from emission factor variability to less than 20% of TC.

Ispra is located to the north of the Po Valley and it is representative of rural/near city areas. In Ispra anthropogenic activities, through fossil fuel and biomass burning, contributed to 92% and 55% of TC during winter and summer, respectively. During the colder months, the largest fraction of the anthropogenic carbon was produced by biomass burning for residential heating (66%). Environmental policies need to take into account the contribution of anthropogenic biomass burning to effectively reduce the concentration of fine particulate mass.

The comparison of source apportionment data with the global chemistry transport model TM5 showed the largest discrepancy in winter POA. The discrepancy was similar to the concentration of primary organic carbon emitted by biomass burning, whose contribution was not included in the model. Ispra, as other European rural areas, showed to be strongly affected by emissions from biomass fuel combustion, most likely wood burning; as a consequence, the availability of up-to-date wood burning emission inventories is a requirement to simulate correctly the OM distribution and eventually to evaluate the efficiency of aerosol reduction strategies. Moreover, TM5 model underestimated biogenic SOA and anthropogenic SOA from oxidation of IVOC.

ACPD
11, 2503–2547, 2011

SOA from anthropogenic activities reported in this study represents a lower estimate of the actual SOA, due to the semi-volatile character of primary organic aerosol, which is not described accurately by the available emission factors. Still, the contribution of SOA from biomass burning and fossil fuel burning was significant: SOA represented 32% and 84% of OM during winter and summer, respectively. These results agree with the high oxidized character of atmospheric organic aerosol reported by Aerodyne Aerosol Mass Spectrometer (AMS) measurements in anthropogenically influenced Northern Hemisphere areas (Zhang et al., 2007).

Biogenic SOA represented a significant percentage of OM both during winter (12%) and summer (61%), while carbon associated to primary biogenic aeorsol was smaller than 1% during the entire year.

In summer the site was affected by polluted air masses from the urban and industrialized areas located in the near Po Valley. The concentration of secondary biogenic aerosol during the same season was enhanced by anthropogenic primary aerosol, in agreement with earlier modeling studies (Tsigaridis and Kanakidou, 2007). In particular, the average concentration of secondary biogenic aerosol would be reduced by about 50% through the removal of anthropogenic primary aerosol. The ultimate consequence of this would be that policies aiming to reduce aerosol species associated with positive warming (e. g. black carbon) would also reduce cooling secondary aerosol.

In closing, we showed that radiocarbon measurements, in combination with tracer analysis, represent a unique tool to constrain the relative contributions of the major sources of carbonaceous aerosols, and that together with trajectory analysis, important information on the source regions can be determined. An expanding dataset is necessary to further understand the world wide contributions of sources to carbonaceous aerosol, improve emission inventories, and provide important information for emission reduction strategies.

ACPD
11, 2503–2547, 2011

Acknowledgements. This work was supported by the European Commission on the IP EU-CAARI (036833-2) project. We gratefully acknolwedge the EMEP team for their dedicated and reliable work during sample collection and M. Duane for skillful assistance in the LC-MS analysis.

References

Aiken, A. C., DeCarlo, P. F., Kroll, J. H., Worsnop, D. R., Huffman, J. A., Docherty, K. S., Ulbrich, I. M., Mohr, C., Kimmel, J. R., Sueper, D., Sun, Y., Zhang, Q., Trimborn, A., Northway, M., Ziemann, P. J., Canagaratna, M. R., Onasch, T. B., Alfarra, M. R., Prevot, A. S. H., Dommen, J., Duplissy, J., Metzger, A., Baltensperger, U., and Jimenez, J. L.: O/C and OM/OC Ratios of Primary, Secondary, and Ambient Organic Aerosols with High-Resolution Time-of-Flight Aerosol Mass Spectrometry, Environ. Sci. Technol, 42, 4478–4485, doi:10.1021/es703009q, 2008. 2522

Bauer, H., Kasper-Giebl, A., Zibuschka, F., Hitzenberger, R., Kraus, G., and Puxbaum, H.: Determination of the carbon content of airborne fungal spores, Anal. Chem., 74, 91–95, 2002. 2513

Bauer, H., Claeys, M., Vermeylen, R., Schueller, E., Weinke, G., Berger, A., and Puxbaum, H.: Arabitol and mannitol as tracers for the quantification of airborne fungal spores, Atmos. Environ., 42, 588–593, 2008a. 2510, 2513, 2521

Bauer, H., Schueller, E., Weinke, G., Berger, A., Hitzenberger, R.and Marr, I., and Puxbaum, H.: Significant contributions of fungal spores to the organic carbon and to the aerosol mass balance of the urban atmospheric aerosol, Atmos. Environ., 42, 5542–5549, 2008b. 2513

Birch, M. E. and Cary, R. A.: Elemental carbon-based method for monitoring occupational exposures to particulate diesel exhaust, Aerosol Sci. Technol., 25, 221–241, 1996. 2509

Bowman, F. M. and Melton, J. A.: Effect of activity coefficient models on predictions of secondary organic aerosol partitioning, J. Aerosol Sci., 35, 1415–1438, 2004. 2523

Boyle, P. P. and Tan, K. S.: Quasi-Monte Carlo methods, International AFIR Colloquium Proceedings, Australia, 1, 1–24, 1997. 2515

Carlton, A. G., Pinder, R. W., Bhave, P. V., and Pouliot, G. A.: To what extent can biogenic SOA be controlled, Environ. Sci. Technol., 44, 3376–3380, 2010. 2523

Cavalli, F., Viana, M., Yttri, K. E., Genberg, J., and Putaud, J.-P.: Toward a standardised

ACPD

11, 2503–2547, 2011

thermal-optical protocol for measuring atmospheric organic and elemental carbon: the EUSAAR protocol, Atmos. Meas. Tech., 3, 79–89, doi:10.5194/amt-3-79-2010, 2010. 2509

Chen, Q., Farmer, D., Schneider, J., Zorn, S., Heald, C., Karl, T., Guenther, A., Allan, J., Robinson, N., Coe, H., Kimmel, J., Pauliquevis, T., Borrmann, S., Poschl, U., Andreae, M., Artaxo, P., Jimenez, J., and Martin, S.: Mass spectral characterization of submicron biogenic organic particles in the Amazon Basin, Geophys. Res. Lett., 36, L20806, doi:10.1029/2009GL039880, 2009. 2524

Colombi, C., Gianelle, V., Belis, C. A., and Larsen, B. R.: Determination of local source profile for soil dust, brake dust, and biomass burning sources, Chemical Engineering Transaction, 22, 233–238, doi:10.3303/CET1022038, 2010. 2517

Currie, L., Stafford, T., Sheffield, A., Klouda, G., Wise, S., Fletcher, R., Donahue, D., Jull, A., and T.W., L.: Microchemical and molecular dating,, Radiocarbon, 31, 448–463, 1989. 2511

Ding, X., Zheng, M., Edgerton, E. S., Jansen, J. J., and Wang, X.: Contemporary or Fossil Origin: Split of Estimated Secondary Organic Carbon in the Southeastern United States, Environ. Sci. Technol, 42, 9122–9128, 2008. 2508

Dixon, R. W. and Baltzell, G.: Determination of levoglucosan in atmospheric aerosols using high performance liquid chromatography with aerosol charge detection, J. Chromatogr., 1109, 214–221, 2006. 2510

Docherty, K. S., Stone, E. A., Ulbrich, I. M., DeCarlo, P. F., Snyder, D. C., Schauer, J. J., Peltier, R. E., Weber, R. J., Murphy, S. M., Seinfeld, J. H., Grover, B. D., Eatough, D. J., and Jimenez, J. L.: Apportionment of Primary and Secondary Organic Aerosols in Southern California during the 2005 Study of Organic Aerosols in Riverside (SOAR-1), Environ. Sci. Technol, 42, 7655–7662, 2008. 2507

Duane, M., Poma, B., Rembges, D., Astorga, C., and Larsen, B. R.: Isoprene and its degradation products as strong ozone precursors in Insubria, Northern Italy, Atmos. Environ., 36, 3867–3879, 2002. 2522

El Haddad, I., Marchand, N., Wortham, H., Piot, C., Besombes, J.-L., Cozic, J., Chauvel, C., Armengaud, A., Robin, D., and Jaffrezo, J.-L.: Primary sources of $PM_{2.5}$ organic aerosol in an industrial Mediterranean city, Marseille, Atmos. Chem. Phys. Discuss., 10, 25435–25490, doi:10.5194/acpd-10-25435-2010, 2010. 2507

Fabbri, D., Torri, C., Simoneit, B. R. T., Marynowski, L., Rushdi, A., and Fabiaska, M. J.: Levoglucosan and other cellulose and lignin markers in emissions from burning of Miocene lignites, Atmos. Environ., 43, 2286–2295, 2009. 2510

ACPD
11, 2503–2547, 2011

Fine, P. M., Cass, G. R., and Simoneit, B. R. T.: Chemical Characterization of Fine Particle Emissions from the Fireplace Combustion of Woods Grown in the Northeastern United States, Environ. Sci. Technol, 35, 2665–2675, 2001. 2517, 2518

Fine, P. M., Cass, G. R., and Simoneit, B. R. T.: Chemical Characterization of Fine Particle Emissions from the Fireplace Combustion of Woods Grown in the Southern United States, Environ. Sci. Technol., 36, 1442–1451, 2002. 2517, 2518

Fine, P. M., Cass, G. R., and Simoneit, B. R. T.: Chemical Characterization of Fine Particle Emissions from the wood stove combustion of prevalent United States tree species, Environmental Engineer Science, 21, 705–721, 2004. 2517

Fraser, M. P. and Lakshmanan, K.: Using levoglucosan as a molecular marker for the long-range transport of biomass combustion aerosols, Environmental Engineer Science, 34, 4560–4564, 2000. 2510

Gelencser, A., May, B., Simpson, D., Sanchez-Ochoa, A., Kasper-Giebl, A., Puxbaum, H., Caseiro, A., Pio, C., and Legrand, M.: Source apportionment of PM2.5 organic aerosol over Europe: Primary/secondary, natural/anthropogenic, and fossil/biogenic origin, J. Geophys. Res., 112, D23S04, doi:10.1029/2006JD008094, 2007. 2508, 2521, 2526

Genberg, J., Stenström, K., Elfman, M., and Olsson, M.: Development of graphitization of μg-sized samples at Lund University, Radiocarbon, 52, 1270–1276, 2010. 2512

Gery, M. W., Whitten, G. Z., and Killus, J. P.: Development and testing of the CBM-IV for urban and regional modelling, EPA-600/3-88-012, Tech. rep., US EPA, Research Triangle Park, 1989. 2523

Hays, M. D., Geron, C. D., Linna, K. J., and Smith, N. D.: Speciation of gas–phase and particle emissions from burning of foliar fuels, Environ. Sci. Technol, 36, 2280–2295, 2002. 2516, 2517

Henne, S., Brunner, D., Folini, D., Solberg, S., Klausen, J., and Buchmann, B.: Assessment of parameters describing representativeness of air quality in-situ measurement sites, Atmos. Chem. Phys., 10, 3561–3581, doi:10.5194/acp-10-3561-2010, 2010. 2509

Hitzenberger, R., Petzold, A., Bauer, H., Ctyroky, P., Pouresmaeil, P., Laskus, L., and Puxbaum, H.: Intercomparison of thermal and optical measurement methods for elemental carbon and black carbon at an urban location., Environ. Sci. Technol, 40, 6377–6383, 2006. 2516

Hodzic, A., Jimenez, J. L., Prévôt, A. S. H., Szidat, S., Fast, J. D., and Madronich, S.: Can 3-D models explain the observed fractions of fossil and non-fossil carbon in and near Mexico City?, Atmos. Chem. Phys., 10, 10997–11016, doi:10.5194/acp-10-10997-2010, 2010. 2507

ACPD
11, 2503–2547, 2011

IPCC: Fourth Assessment Record: Climate change 2007, Cambridge University Press, New York, 2007. 2506

Jia, Y., Bhat, S., and Fraser, M. P.: Characterization of saccharides and other organic compounds in fine particles and the use of saccharides to track primary biologically derived carbon sources, Atmos. Environ., 44, 724–732, 2010. 2510, 2521

Karl, M., Tsigaridis, K., Vignati, E., and Dentener, F.: Formation of secondary organic aerosol from isoprene oxidation over Europe, Atmos. Chem. Phys., 9, 7003–7030, doi:10.5194/acp-9-7003-2009, 2009. 2522, 2523

Kourtchev, I., Copolovici, L., Claeys, M., and Maenhaut, W.: Characterization of atmospheric aerosols at a forestd site in central Europe, Environ. Sci. Technol, 43, 4665–4671, 2009. 2521

Krol, M., Houweling, S., Bregman, B., van den Broek, M., Segers, A., van Velthoven, P., Peters, W., Dentener, F., and Bergamaschi, P.: The two-way nested global chemistry-transport zoom model TM5: algorithm and applications, Atmos. Chem. Phys., 5, 417–432, doi:10.5194/acp-5-417-2005, 2005. 2523

Kuo, L. J., Herbert, B. E., and Louchouarn, P.: Can levoglucosan be used to characterize and quantify char/charcoal black carbon in environmental media?, Organic Geochemistry, 39, 1466–1478, 2008. 2510

Kupiainen, K. and Klimont, Z.: Primary emissions of submicron and carbonaceous particles in Europe and the potential for their control, Tech. Rep. IR-04-079, International Institute for Applied System analysis IIASA, 2004. 2517

Kupiainen, K. and Klimont, Z.: Primary emissions of fine carbonaceous particles in Europe, Atmos. Environ., 41, 2156–2170, 2007. 2517

Lal, D. and Peters, B.: Cosmic ray produces radioactivity on the Earth, Handbuch der Physik, 46, 551–612, 1967. 2507

Lee, S., Wang, Y., and Russell, A. G.: Assessment of secondary organic carbon in the southestern United States: a review, Air Waste Manage. Assoc., 60, 1282–1292, 2010. 2507, 2508

Levin, I. and Kromer, B.: The tropospheric $^{14}CO_2$ level in mid-latitudes of the northern hemisphere (1959–2003), Radiocarbon, 46, 1261–1272, 2004. 2511

Levin, I. Hammer, S., Kromer, B., and Meinhardt, F.: Radiocarbon observations in atmopsheric CO_2: determining fossil fuel CO_2 over Europe using Jungfraujoch observations as background, Sci. Total Environ., 391, 211–216, 2008. 2511, 2514

ACPD

11, 2503–2547, 2011

Lewis, C. W., Klouda, G. A., and Ellenson, W. D.: Radiocarbon measurenents of the biogenic contribution to summertime PM2.5 ambient aerosol in Nashville, TN, Atmos. Environ., 38, 6053–6061, 2004. 2518

Lonati, G., Giugliano, M., Butelli, P., Romele, L., and Tardivo, R.: Major chemical components of PM2.5 in Milan (Italy), Atmos. Environ., 39, 1925–1934, 2005. 2517

Ma, Y., Hays, M. D., Geron, C. D., Walker, J. T., and Gatari Gichuru, M. J.: Technical Note: Fast two-dimensional GC-MS with thermal extraction for anhydro-sugars in fine aerosols, Atmos. Chem. Phys., 10, 4331–4341, doi:10.5194/acp-10-4331-2010, 2010. 2511

Matthias-Maser, S. and Jaenicke, R.: The size distribution of primary biological aerosol particles in the multiphase atmosphere, Aerobiologia, 16, 207–210, 2000. 2513

Nel, A.: Air pollution – related illness: Effects of particles, Science, 308, 5723, doi:10.1126/science.1108752, 2005. 2506

Nolte, C. G., Schauer, J. J., Cass, G. R., and Simoneit, B. R. T.: Highly polar organic compounds present in wood smoke and in the ambient atmosphere, Environ. Sci. Technol., 35, 1912–1919, 2001. 2510

Pekneya, N., Davidsonb, C. I., Zhouc, L., and Hopkec, P. K.: Application of PSCF and CPF to PMF-Modeled Sources of $PM_{2.5}$ in Pittsburgh, Aerosol Sci. Technol., 40, 952–961, 2004. 2519

Pope, C. A. r. and Dockery, C. W.: Health effects of fine particulate air pollution: Lines that connect, J. Air Waste Manage. Assoc., 56, 709–742, 2006. 2506

Puxbaum, H., Caseiro, A., Sanchez-Ochoa, A., Kasper-Giebl, A., Claeys, M., Gelencser, A., Legrand, M., Preunkert, S., and Pio, C.: Levoglucosan levels at background sites in Europe for assessing the impct of biomass combustion on the European aerosol background, J. Geophys. Res, 112, D23S05, doi:10.1029/2006JD008114, 2007. 2517, 2521, 2522

Querol, X., Alastuey, A., Pey, J., Cusack, M., Pérez, N., Mihalopoulos, N., Theodosi, C., Gerasopoulos, E., Kubilay, N., and Koçak, M.: Variability in regional background aerosols within the Mediterranean, Atmos. Chem. Phys., 9, 4575–4591, doi:10.5194/acp-9-4575-2009, 2009. 2506

Robinson, A., Donahue, N. M., Shrivastava, M. K., Weitkamp, E. A., Sage, A. M., Grieshop, A. P., Lane, T. E., Pierce, J. R., and Pandis, S.: Rethinking organic aerosols: semivolatile emissions and photochemical aging, Science, 315, 1259–1262, 2007. 2514, 2518

Schauer, J. J., Kleeman, M. J., Cass, G. R., and Simoneit, B. R. T.: Measurement of emissions from air pollution sources. 3 C1–C29 organic compounds from fireplace combstion of wood,

ACPD
11, 2503–2547, 2011

Environ. Sci. Technol., 35, 1716–1728, 2001. 2516
Schmidl, C., Marr, I. L., Caseiro, A., Kotianova, P., Berner, A., Bauer, H., Kasper-Giebl, A., and Puxbaum, H.: Chemical characterization of fine particle emissions from wood stove combustion of common woods growing in the mid-European Alpine regions, Atmos. Environ., 42, 126–141, 2008a. 2510, 2517
Schmidl, C., Bauer, H., Dattler, A., Hitzenberger, R., Weissenboeck, G., Marr, I. L., and Puxbaum, H.: Chemical characterization of particle emissions from burning leaves, Atmos. Environ., 42, 9070–9079, 2008b.
Simoneit, B. R. T., Elias, V. O., Kobayashi, M., Kawamura, K., Rushdi, A., Medeiros, P. M., Rogge, W. F., and Didyk, B. M.: Sugars-Dominant Water-Soluble Organic Compounds in Soils and Characterization as Tracers in Atmospheric Particulate Matter, Environ. Sci. Technol., 38, 5939–5949, 2004. 2510
Skog, G.: The single stage AMS machine at Lund University: Status Report, Nuclear Instruments and Methods B, 259, 1–6, 2007. 2512
Skog, G., Rundgren, M., and Sköld, P.: Status of the Single Stage AMS machine at Lund University after 4 years of operation, Nuclear Instruments and Methods B, 268, 895–897, 2010. 2512
Sobol, I. M.: The distribution of points in a cube and the approximate evaluation of integrals, U.S.S.R. Computational mathematics and mathematical physics, 1967. 2515
Stohl, A., Wotawa, G., Seibert, P., and Kromp-Kolb, H.: Interpolation Errors in Wind Fields as a Function of Spatial and Temporal Resolution and Their Impact on Different Types of Kinematic Trajectories, J. Appl. Meteorol., 34, 2149–2165, 1995. 2518
Stohl, A., Forster, C., Frank, A., Seibert, P., and Wotawa, G.: Technical note: The Lagrangian particle dispersion model FLEXPART version 6.2, Atmos. Chem. Phys., 5, 2461–2474, doi:10.5194/acp-5-2461-2005, 2005. 2518
Stone, E. A., Snyder, D. C., Sheesley, R. J., Sullivan, A. P., Weber, R. J., and Schauer, J. J.: Source apportionment of fine organic aerosol in Mexico City during the MILAGRO experiment 2006, Atmos. Chem. Phys., 8, 1249–1259, doi:10.5194/acp-8-1249-2008, 2008. 2507
Szidat, S., Prévôt, A. S. H., Sandradewi, J., Alfarra, M. R., Synal, H.-A., Wacker, L., and Baltensperger, U.: Dominant impact of residential wood burning on particulate matter in Alpine valleys during winter, Geophys. Res. Lett., 34, L05820, doi:10.1029/2006GL028325, 2007. 2507, 2526
Szidat, S., Ruff, M., Perron, N., Wacker, L., Synal, H.-A., Hallquist, M., Shannigrahi, A. S.,

ACPD
11, 2503–2547, 2011

Yttri, K. E., Dye, C., and Simpson, D.: Fossil and non-fossil sources of organic carbon (OC) and elemental carbon (EC) in Göteborg, Sweden, Atmos. Chem. Phys., 9, 1521–1535, doi:10.5194/acp-9-1521-2009, 2009. 2508

Tsigaridis, K. and Kanakidou, M.: Secondary organic aerosol importance in the future atmosphere, Atmos. Environ., 41, 4682–4692, cited By (since 1996) 37, 2007. 2529

Tsigaridis, K., Krol, M., Dentener, F. J., Balkanski, Y., Lathière, J., Metzger, S., Hauglustaine, D. A., and Kanakidou, M.: Change in global aerosol composition since preindustrial times, Atmos. Chem. Phys., 6, 5143–5162, doi:10.5194/acp-6-5143-2006, 2006. 2523

Wan, E. C. and Yu, J. Z.: Determination of sugar compounds in atmospheric aerosols by liquid chromatography combined with positive electrospray ionization mass spectrometry, J. Chromatogr., 1107, 175–181, 2006. 2510

Watson, J. G. and Chow, J. C.: Source characterization of major emission sources in the Imperial and Mexicali Valleys along the US/Mexico border, Sci. Total Environ., 276, 33–47, 2001. 2517

Yu, X.-Y., Cary, R. A., and Laulainen, N. S.: Primary and secondary organic carbon downwind of Mexico City, Atmos. Chem. Phys., 9, 6793–6814, doi:10.5194/acp-9-6793-2009, 2009. 2507

Zdráhal, Z., Oliveira, J., Vermeylen, R., Claeys, M., and Maenhaut, W.: Improved method for quantifying levoglucosan and related monosaccharide anhydrides in atmospherc aerosols and application to samples from urban and tropical locations, Environ. Sci. Technol., 36, 747–753, 2002. 2510

Zeng, Y. and Hopke, P. K.: Study of the sources of acid precipitation in Ontario, Canada, Atmos. Environ., 23, 1499–1509, 1989. 2519

Zhang, Q., Jimenez, J. L., Canagaratna, M. R., Allan, J. D., Coe, H., Ulbrich, I., Alfarra, M. R., Takami, A., Middlebrook, A. M., Sun, Y. L., Dzepina, K., Dunlea, E., Docherty, K., DeCarlo, P. F., Salcedo, D., Onasch, T., Jayne, J. T., Miyoshi, T., Shimono, A., Hatakeyama, S., Takegawa, N., Kondo, Y., Schneider, J., Drewnick, F., Borrmann, S., Weimer, S., Demerjian, K., Williams, P., Bower, K., Bahreini, R., Cottrell, L., Griffin, R. J., Rautiainen, J., Sun, J. Y., Zhang, Y. M., and Worsnop, D. R.: Ubiquity and dominance of oxygenated species in organic aerosols in anthropogenically-influenced Northern Hemisphere midlatitudes, Geophys. Res. Lett., 34, L13801, doi:10.1029/2007GL029979, 2007. 2506, 2529

ACPD
11, 2503–2547, 2011

Table 1. List of acronyms used in the paper and the corresponding descriptions.

Acronym	Description
POC_{bb}	Biomass burning primary OC
SOC_{bb}	Biomass burning secondary OC
EC_{bb}	Biomass burning EC
POC_{bio}	Biogenic primary OC
SOC_{bio}	Biogenic secondary OC
POC_{ff}	Fossil fuel burning primary OC
SOC_{ff}	Fossil fuel burning secondary OC
EC_{ff}	Fossil fuel burning EC
$f_{M(non-fossil)}$	Reference fraction of modern carbon of non-fossil aerosol
$f_{M(bb)}$	Reference fraction of modern carbon of biomass burning aerosol
$f_{M(bio)}$	Reference fraction of modern carbon of biogenic aerosol

ACPD
11, 2503–2547, 2011

Table 2. Variability ranges of the input parameters used in the Quasi Monte Carlo simulations.

Parameter	Lower bound	Upper bound
OC to levoglucosan ratio	4	6
OC to EC ratio–bb	1	20
OC to EC ratio–ff	0.3	1.2
$f_{M(bb)}$	1.13	1.31
$f_{M(non-fossil)}$	1.05	$f_{M(bb)}$

ACPD
11, 2503–2547, 2011

Table 3. Annual and seasonal average concentrations of $PM_{2.5}$, OC, EC, corresponding to the entire set of samples collected during 2007 (upper part) together with $PM_{2.5}$, OC, EC levoglucosan, arabitol, and mannitol averages corresponding to the subset of 48 samples (lower part). Concentrations are in $\mu g\,m^{-3}$ and standard deviations are reported; averages are calculated using non-null values, whose number is reported between brackets.

Species	Entire year	Winter (Jan–Mar Oct–Dec)	Summer (Apr–Sep)
$PM_{2.5}$	25.7 ± 21.4 (322)	37.3 ± 23.6 (166)	13.5 ± 8.4 (156)
OC	9.2 ± 8.5 (334)	14.1± 9.2 (173)	4.0 ± 2.4 (161)
EC	2.3 ± 2.2 (334)	3.7 ± 2.3 (173)	0.9 ± 0.5 (161)
$PM_{2.5}$	35.9 ± 22.6 (49)	48.1 ± 27.3 (28)	19.6 ± 9.3 (21)
OC	13.8 ± 10.1 (49)	19.5 ± 10.2 (28)	6.3 ± 3.1 (21)
EC	3.5 ± 2.6 (49)	5.1 ± 13.0 (28)	1.4 ± 0.9 (21)
Levoglucosan	2.5 ± 1.9 (33)	2.8 ± 5.4 (28)	0.5 ± 0.3 (5)
Arabitol*	9.9 ± 7.6 (49)	10.2 ± 12.1 (12)	7.5 ± 2.1 (2)
Mannitol*	11.6 ± 14.6 (14)	14.0 ± 59.2 (12)	4.2 ± 2.6 (4)

* Arabitol and mannitol concentrations are in $ng\,m^{-3}$.

ACPD
11, 2503–2547, 2011

Table 4. Annual and seasonal average carbon concentrations (in $\mu g\,m^{-3}$) of the Quasi Monte Carlo best estimate results, and corresponding fraction of carbon mass between brackets.

Source	Entire year	Winter (Jan–Mar Oct–Dec)	Summer (Apr–Sep)
POC_{bb}	7.0 (40%)	12.3 (50%)	0.5 (6%)
SOC_{bb}	0.7 (4%)	1.8 (7%)	0.3 (4%)
EC_{bb}	1.1 (6%)	2.3 (9%)	0.1 (2%)
POC_{bio}	<0.1	<0.1	<0.1
SOC_{bio}	2.7 (15%)	1.9 (8%)	3.4 (45%)
POC_{ff}	1.0 (6%)	1.3 (5%)	0.7 (9%)
SOC_{ff}	1.5 (9%)	2.2 (9%)	1.4 (18%)
EC_{ff}	2.2 (13%)	2.8 (12%)	1.2 (16%)

ACPD
11, 2503–2547, 2011

Table 5. Percentage values of TC emitted by biomass burning (bb), fossil fuel burning (ff) and biogenic (bio) sources as OC and EC.

Site	Notes	OC_{bb}	EC_{bb}	OC_{ff}	EC_{ff}	OC_{bio}	Reference
Winter							
Aveiro	Rural	64[a]	11	17	2		Gelencser et al. (2007)
K-Puszta	Rural	40[a]	7	21	10		Gelencser et al. (2007)
Rao	Rural	31	8	28	16	17	Szidat et al. (2009)
Roveredo	Rural	75[b]	11	4	12		Szidat et al. (2007)
Roveredo	Rural	62[b]	8	21	11		Szidat et al. (2007)
Moleno	Rural	54[b]	4	15	30		Szidat et al. (2007)
Zurich	Urban	29	4	25	16	46	Szidat et al. (2006)
Göteborg	Urban	20	3	28	26	23	Szidat et al. (2009)
Ispra		57	9	14	12	8	This study
Summer							
Aveiro	Rural	7[c]	1	7	13	65[c]	Gelencser et al. (2007)
K-Puszta	Rural	6[c]	1	9	9	69[c]	Gelencser et al. (2007)
Zurich	Urban	8	1	24	22	46	Szidat et al. (2006)
Göteborg	Urban	9	2	31	15	44	Szidat et al. (2009)
Ispra		10	2	27	16	45	This study

[a] Neglecting secondary OC;

[b] Assuming non-fossil OC was OC_{bb} in winter;

[c] Assuming secondary non-fossil OC was OC_{bio} in summer.

ACPD
11, 2503–2547, 2011

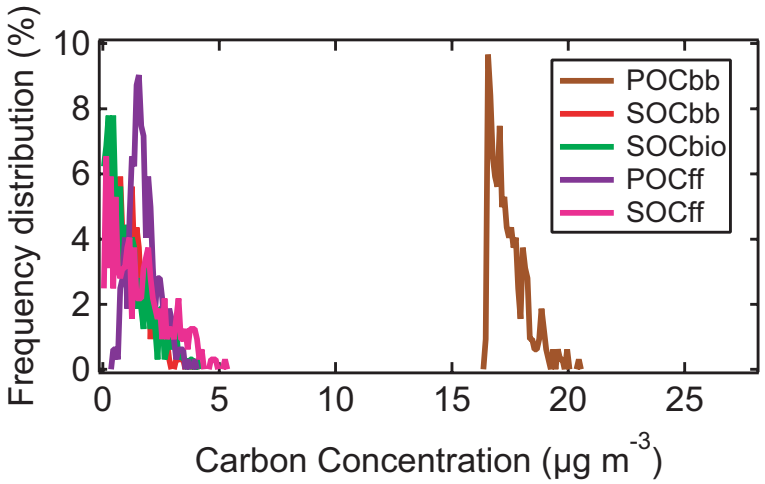

Fig. 1. Example of QMC solution frequency distributions corresponding to primary and secondary OC concentrations; EC frequency distributions are not reported for simplicity.

ACPD
11, 2503–2547, 2011

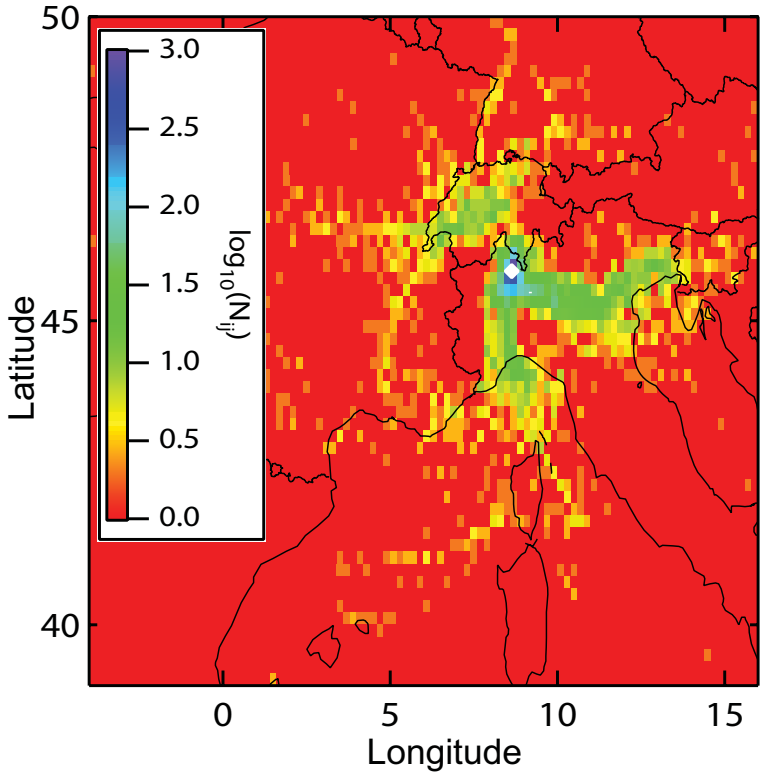

Fig. 2. Frequency distribution map (on a logarithmic scale) of back trajectory passes during aerosol collection periods.

ACPD
11, 2503–2547, 2011

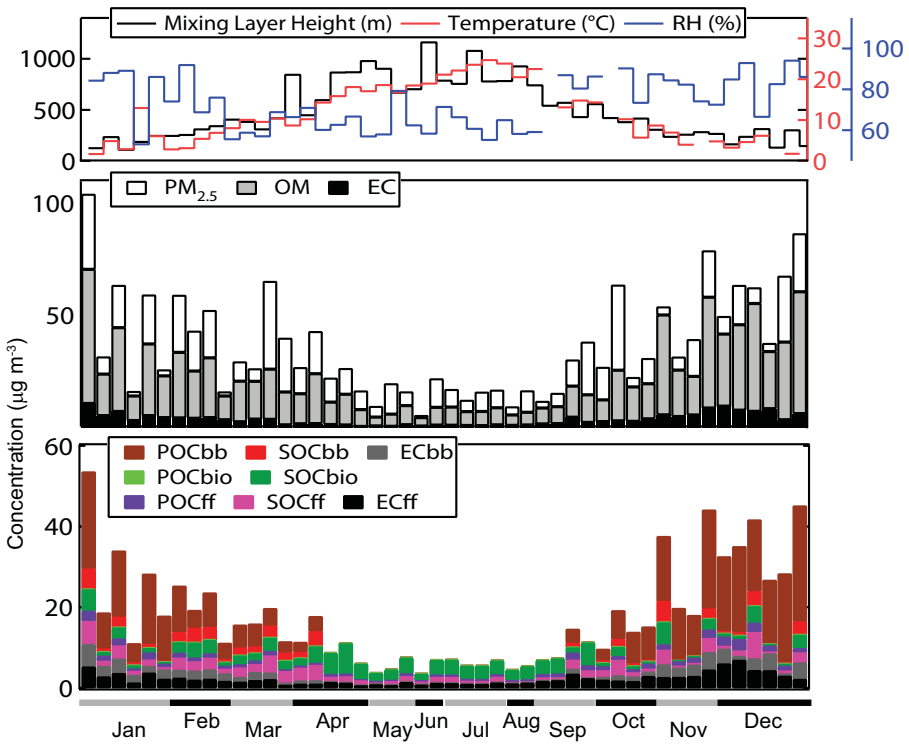

Fig. 3. Meteorological parameters **(a)**, contribution of OC and EC to $PM_{2.5}$ **(b)**, and best estimate results of source apportionment study **(c)** corresponding to the subset of daily aerosol samples here investigated.

ACPD
11, 2503–2547, 2011

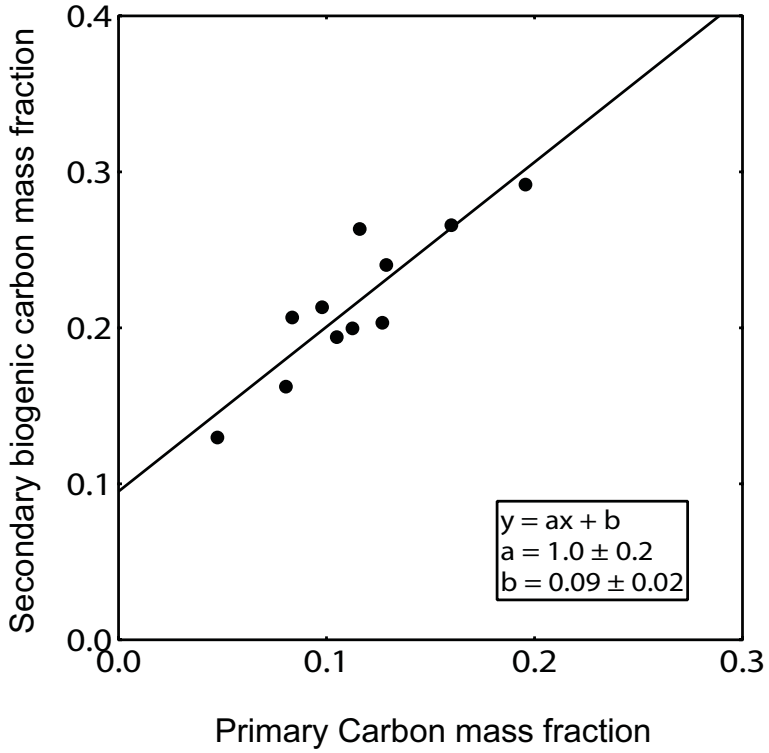

Fig. 4. Biogenic secondary carbon relative to primary anthropogenic carbon concentration during May–August.

ACPD
11, 2503–2547, 2011

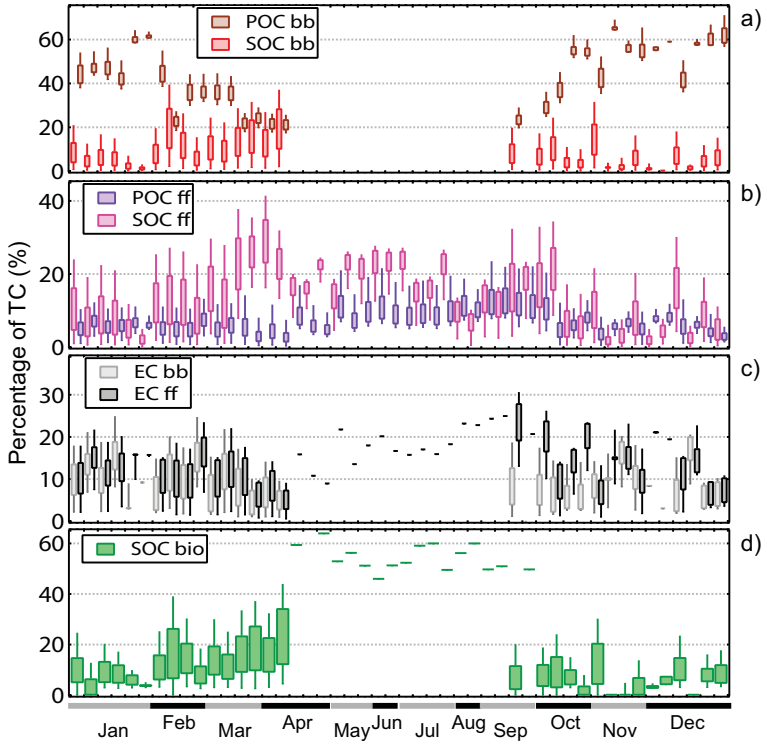

Fig. 5. Box-whisker plots of Quasi Monte Carlo simulation output for each day and each carbon source: POC_{bb} and SOC_{bb} **(a)**, POC_{ff} and SOC_{ff} **(b)**, EC_{bb} and EC_{ff} **(c)**, and SOC_{bio} **(d)**.

ACPD
11, 2503–2547, 2011

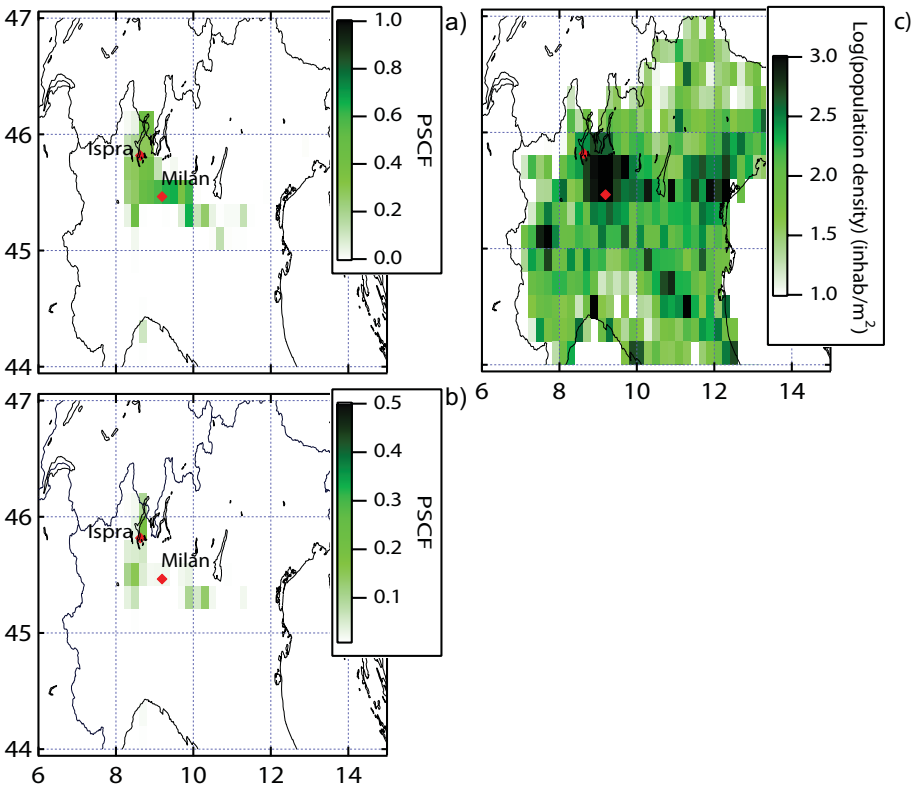

Fig. 6. PSCF maps of fossil fuel combustion **(a)** and biomass burning **(b)** aerosol; **(c)** shows northern Italy population density (ISTAT 2005).

ACPD
11, 2503–2547, 2011